Nanoscale Horizons

ROYAL SOCIETY OF CHEMISTRY

COMMUNICATION

View Article Online
View Journal | View Issue

Cite this: *Nanoscale Horiz.*, 2025, **10**, 2615

Received 28th May 2025,
Accepted 31st July 2025

DOI: 10.1039/d5nh00367a

rsc.li/nanoscale-horizons

Tunable directional thermal emission using a phase change material-based multilayer structure

Kandammathe Valiyaveedu Sreekanth, *[ab] Qing Yang Steve Wu,[a] Sambhu Jana,[cd] Ranjan Singh[e] and Jinghua Teng *[ab]

The directional and spectral control of thermal emission with a tunable angular range is essential for realizing next-generation smart thermal emitters. However, existing photonic strategy-based thermal emitters manage thermal emission only over a fixed angular range. Here, we present a lossless chalcogenide phase change material (PCM)-based tunable multilayer structure as a thermal emitter for actively regulating angular selectivity in thermal emission. We develop a tunable multilayer stack with a thickness of 1.35 μm by layering alternating thin films of SiO_2 and a high-crystallization-temperature PCM, such as Sb_2S_3. The principle underlying the proposed tunable directional control of thermal emission relies on the tunable Brewster mode within the SiO_2–Sb_2S_3 multilayer cavity. For *p*-polarized light, the cavity exhibits maximum emissivity across a broad spectral band (10–18 μm) around the Brewster angle. In particular, a peak emissivity of over 95% is achieved in this broad spectral band at the Brewster angle. The angular range of maximum thermal emission can be tuned through the non-volatile structural phase transition property of Sb_2S_3, while maintaining a constant spectral bandwidth. Moreover, we demonstrate electrically controlled thermal emission using a microheater-integrated Sb_2S_3–SiO_2 multilayer cavity. This photonic structure could serve as a versatile, tunable, lithography-free platform to dynamically control the angular range of directional thermal emission and emissivity for emerging applications of thermal emitters.

New concepts

Since thermal emission is a broadband phenomenon, controlling the directionality (angular selectivity) of emitted far-field thermal radiation presents a fundamental challenge. Although directional control of thermal emission has been achieved using various photonic structures, tunable angular selectivity has not been extensively studied. Recently, the thermally tunable angular selectivity of broadband directional thermal emission was demonstrated using InAs-based gradient epsilon-near-zero (ENZ) materials (*Nano Lett.*, 2025, **25**, 8064–8071). However, InAs is a volatile material that shows low refractive index variation with temperature. In this work, we propose a multilayer structure based on a chalcogenide phase change material (PCM), such as Sb_2S_3, to enable tunable directional control of thermal emission. Sb_2S_3 is a non-volatile material that exhibits a substantial change in refractive index by switching from amorphous to crystalline phase through thermal treatment. Consequently, the proposed photonic structure provides greater angular tunability compared to existing methods. This is the first demonstration of a PCM-based tunable multilayer cavity for adjustable directional control of thermal emission. Additionally, we report electrically controlled thermal emission using a compact microheater integrated cavity. Achieving angular-selective thermal emission across a broad spectrum is vital for numerous applications, especially in daytime radiative cooling.

1. Introduction

Thermal radiation is a broadband phenomenon that presents a fundamental challenge in controlling the directionality (angular selectivity) of the emitted far-field thermal radiation.[1] The directional and spectral control of thermal emission across a wide bandwidth is crucial for applications such as thermal camouflaging, solar heating, radiative cooling, and waste heat recovery.[2–7] Notably, angular selective thermal emission has been explored as an additional design factor for daytime radiative cooling, with theoretical studies[8] demonstrating improved cooling performance, especially in humid conditions where atmospheric transmission is reduced. The introduction of selectivity, whether spectral or angular, aims to engineer the emissivity of the thermal emitter to maximize net radiated thermal emission. The thermal emitter exhibits high emissivity at wavelengths and angles with

[a] *Institute of Materials Research and Engineering, Agency for Science, Technology and Research (A*STAR), 2 Fusionopolis Way, Innovis #08-03, Singapore 138634, Republic of Singapore. E-mail: sreekanth@imre.a-star.edu.sg, jh-teng@imre.a-star.edu.sg*
[b] *National Semiconductor Translation and Innovation Centre (NSTIC), 1 Fusionopolis Way, #19-10 Connexis North, Singapore 138632, Republic of Singapore*
[c] *Division of Physics and Applied Physics, School of Physical and Mathematical Sciences, Nanyang Technological University, Singapore 637371, Singapore*
[d] *Centre for Disruptive Photonic Technologies, The Photonics Institute, Nanyang Technological University, Singapore 637371, Singapore*
[e] *Department of Electrical Engineering, University of Notre Dame, Notre Dame, IN, 46556, USA*

significant atmospheric transparency and near-zero emissivity at other wavelengths and angles. The advantage of angular selectivity is that it increases the net radiated power ($Q_{net}(T) = Q_{sample}(T) - Q_{atm}(T_{atm}) - Q_{sun} - Q_{parasitic}$) by blocking solar irradiance (Q_{sun}), enhancing the radiated power from the sample due to omnidirectional thermal emission (Q_{sample}), and reducing the absorbed radiation from the atmosphere (Q_{atm}), since the atmosphere's emissivity rises at higher angles (measured from the zenith).[8] Moreover, tunable directional thermal emission is essential when atmospheric conditions change. Recently, a micro-wedge geometry was proposed to achieve daytime radiative cooling for outdoor vertical surfaces experimentally, resulting in a 2 °C temperature reduction compared to isotropic emitters through directional thermal emission across a broad bandwidth.[9] Additionally, directional emission with narrow spectral bands is crucial for developing efficient infrared light sources, as directionality can significantly enhance energy conversion efficiency.[10]

Various photonic strategies have been proposed to control thermal emission over a fixed narrow angular range; however, these systems only operate within a limited spectral band.[11] Incorporating a functional material into the thermal emitter offers additional control, such as tuning the spectral band and adjusting the emission intensity.[12,13] The tuning of the thermal emission's spectral bandwidth has been demonstrated using phase change materials,[14] thermo-optical modulation,[15] electrostatic gating,[16] magneto-optical materials,[17] and photon chemical potential.[18] Additionally, spectral bandwidth tuning of thermal emission with infrared light emission at specific wavelengths was achieved using catalytic photonic crystals.[19] Recently, broadband directional and spectral control of thermal emission has been experimentally demonstrated with gradient epsilon-near-zero photonic structures (thin film stacks).[20,21] Broadband, unidirectional, and asymmetric thermal emission has also been shown using metasurface-based structures.[22,23] Furthermore, broadband directional thermal emission with emissivity switching has been demonstrated using thermo-optic effects.[12,24–26] However, these systems do not maintain the wavelength range of maximum emissivity when the directional response is adjusted. Recently, an InAs-based gradient epsilon-near-zero platform was proposed to enable tunable directional thermal emission for *p*-polarized light, based on the thermo-optic effect.[27] Since this effect only induces small, volatile changes in the refractive index, angular tunability remains limited. Additionally, this photonic structure exhibits directional emission over a narrow spectral band, spanning from 12.5 to 15 μm. In this context, thermal emission with a tunable angular range and broad spectral bandwidth is essential for advancing next-generation smart thermal emitters for thermal management applications.

Here, we experimentally demonstrate a tunable angular range for broadband directional thermal emission using a chalcogenide phase change material (PCM)-based tunable multilayer structure. PCMs are thermally tunable optical materials that provide stable and power-efficient multistate and non-volatile tunability by altering their structural phase between amorphous and crystalline.[28,29] We utilize the tunable Brewster angle, supported by a PCM-based multilayer cavity, to achieve control over the directionality of thermal emission across a broad spectral band (10–18 μm). Additionally, we develop a compact microheater-integrated multilayer cavity for electrically controlled thermal emission. Importantly, only a thin film deposition technique is needed to create the proposed tunable thermal emitter, enabling wafer-scale fabrication at a low cost.

2. Design and tuning mechanism

Fig. 1a illustrates the designed PCM-based multilayer structure for achieving tunable directional thermal emission, which consists of ten alternating periodic thin layers of SiO_2 and Sb_2S_3 PCM. Note that Sb_2S_3 is a suitable chalcogenide PCM for tunable infrared photonics applications because it exhibits a high refractive index contrast and lossless feature in both amorphous and crystalline phases.[30] Moreover, the crystallization temperature of Sb_2S_3 is higher than that of prototype PCMs, such as $Ge_2Sb_2Te_5$, which is approximately 280 °C. Additionally, the optical constants of the Sb_2S_3 thin film can only be altered by annealing at temperatures of 180 °C or higher.[31,32] This characteristic is essential for PCM-based tunable thermal photonics applications.

According to Kirchhoff's law of thermal radiation, the emissivity (E) for each frequency, polarization, and angle of incidence equals the absorptivity (A), meaning $E(\omega, \theta) = A(\omega, \theta)$. The developed SiO_2–Sb_2S_3 multilayer is opaque to wavelengths greater than 5 μm because SiO_2 layers are not transparent. This indicates that absorptivity can be controlled by managing angular reflection (R), resulting in $A = 1 - R$. Therefore, angular thermal emission can be calculated by determining angular reflection. The principle behind the proposed tunable directional control of thermal emission is based on the tunable Brewster mode in the SiO_2–Sb_2S_3 multilayer. According to the Brewster mode concept, *p*-polarized light should not reflect at the Brewster angle, defined as $\theta_B = \tan^{-1}(\varepsilon_2/\varepsilon_1)^{1/2}$, where θ_B represents the Brewster angle and (ε_2, ε_1) are the dielectric

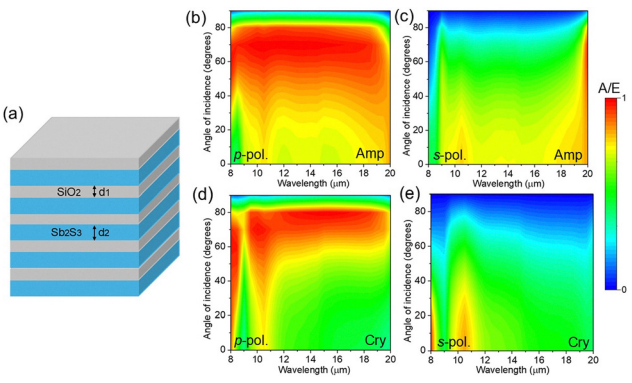

Fig. 1 (a) Schematic of the proposed SiO_2–Sb_2S_3 tunable thermal emitter. Calculated angular absorption spectra of the SiO_2–Sb_2S_3 cavity for the amorphous (Amp) phase of Sb_2S_3: (b) *p*-polarization and (c) *s*-polarization, and for the crystalline (Cry) phase of Sb_2S_3: (d) *p*-polarization and (e) *s*-polarization.

permittivities of the two layers in the periodic multilayer. Generally, *p*-polarized light is fully transmitted for all frequencies at both interfaces (from ε_1 to ε_2 layers and from ε_2 to ε_1 layers). As transmission is zero for wavelengths greater than 5 μm, *p*-polarized light is absorbed at the Brewster angle. Consequently, directional control of thermal emission is possible for an angular range close to the Brewster angle for *p*-polarized light. Moreover, this narrow angular range can be dynamically tuned by altering the permittivity of one of the layers in the multilayer. Here, we adjust the permittivity of the Sb_2S_3 layers by changing the phase of Sb_2S_3 from amorphous to crystalline.

3. Results and discussion

3.1. Numerical simulation results

We used the transfer matrix method[33] to calculate the angular reflectance of the designed multilayer structure. To maximize thermal emission over a broad spectral band, the optimal thicknesses of SiO_2 and Sb_2S_3 are set to 100 nm (d_1) and 170 nm (d_2), respectively. The optical constants (n and k) of SiO_2 and Sb_2S_3 for infrared wavelengths are taken from ref. [34] and ref. [30], respectively. The engineered periodic SiO_2–Sb_2S_3 multilayer acts as a distributed Bragg reflector (DBR), showing photonic band gaps (PBG) in the visible and near-infrared wavelengths (see Fig. S1, SI). The calculated angular absorption ($A = 1 - R$) spectra of the SiO_2–Sb_2S_3 multilayer in both phases of Sb_2S_3 for *p*- and *s*-polarizations are shown in Fig. 1. The absorption spectrum of the amorphous cavity for *p*- and *s*-polarizations is displayed in Fig. 1b and c, respectively. Maximal absorption or emissivity across a broad bandwidth (10–18 μm) for *p*-polarized light occurs within an angular range of 55°–80°, with peak emission (>95%) at the Brewster angle of 70°. However, no such emissivity response is seen for *s*-polarization. After the structural phase transition of Sb_2S_3 from amorphous to crystalline (Fig. 1d and e), the angular range for maximum broadband thermal emission narrows to 65°–80°, with peak emission (>95%) at the Brewster angle of 77° for *p*-polarization. This method allows tuning the angular range of broadband thermal emission, enabling tunable directional thermal emission.

3.2. Experimental results

We fabricated the thermal emitter by depositing an appropriate number of alternating thin layers of Sb_2S_3 and SiO_2 on a quartz substrate. Fig. 2a shows the scanning electron microscope (SEM) image of the fabricated SiO_2–Sb_2S_3 multilayer, labelled from 1 to 10. The stack consists of ten alternating layers of SiO_2 and Sb_2S_3. Thin films of Sb_2S_3 and SiO_2 were deposited using RF magnetron sputtering. Room temperature deposition was conducted in a high-purity argon (99.999%) atmosphere at a deposition pressure of 10 mTorr. The thickness of the grown films was determined using a spectroscopic ellipsometer (V-VASE). Normal incidence reflection and transmission measurements were performed using a microscope-based Fourier-transform infrared

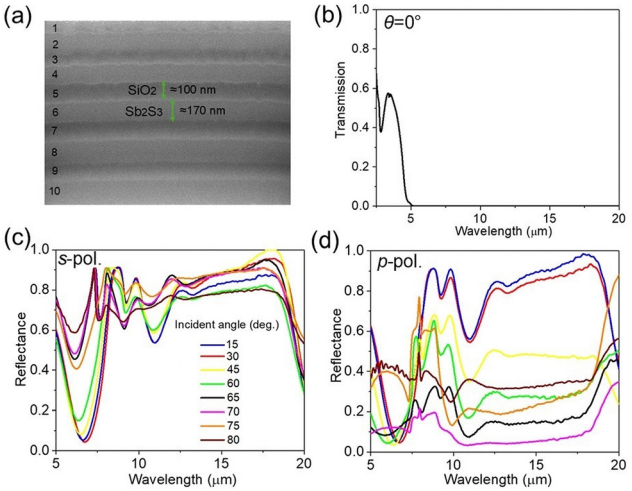

Fig. 2 (a) SEM image of the fabricated SiO_2–Sb_2S_3 multilayer structure. (b) Measured normal incidence transmission spectrum of the amorphous SiO_2–Sb_2S_3 multilayer. Measured angular reflectance spectra of the amorphous SiO_2–Sb_2S_3 multilayer for (c) *s*-polarization and (d) *p*-polarization.

spectroscopy (FTIR) system (Bruker Hyperion 2000), with glow bars as the illumination source and a liquid-nitrogen-cooled MCT detector. Angular reflection measurements for both *p*- and *s*-polarizations were performed using an FTIR system (Bruker Vertex 80 V) equipped with an automated polarization-controlled stage.

Fig. 2b presents the measured normal incidence transmission spectrum of the SiO_2–Sb_2S_3 multilayer in the amorphous phase. As observed, the transmitted intensity is zero for wavelengths greater than 5 μm, indicating that the angular absorption/emissivity can be directly obtained by measuring the angular reflectance. We focus on the thermal emission in the wavelength range of 5–20 μm because the peak of a black body thermal emission spectrum occurs within this spectral band at terrestrial temperatures (approximately 300 K), as predicted by Planck's law of thermal radiation. The measured angular (15–80 degrees) reflectance spectra of the SiO_2–Sb_2S_3 multilayer for *s*- and *p*-polarization are shown in Fig. 2c and d, respectively. The effect of Brewster angle on the SiO_2–Sb_2S_3 multilayer structure is evident from the *p*-polarized reflectance (Fig. 2d), where angle-dependent reflectance demonstrates a minimum reflectance over a wide bandwidth (10 to 18 μm) at an incident angle of 70° (Brewster angle). However, angle-independent higher reflectance is achieved for *s*-polarization within the same spectral band (Fig. 2c). The observed minimum reflectance within the 5 to 8 μm wavelength range for both *p*- and *s*-polarization results from the phonon resonance of SiO_2.

To achieve tunable directional control of broadband thermal emission, the cavity is annealed at 280 °C, causing the phase of the Sb_2S_3 layers to transition from amorphous to crystalline. The phase change is further confirmed using X-ray diffraction (XRD) and Raman measurements (see Fig. S2, SI). Fig. 3a and b present the measured *p*-polarized angular absorption/emissivity spectra of the amorphous and crystalline cavities, respectively. For the amorphous cavity, the peak broadband emissivity

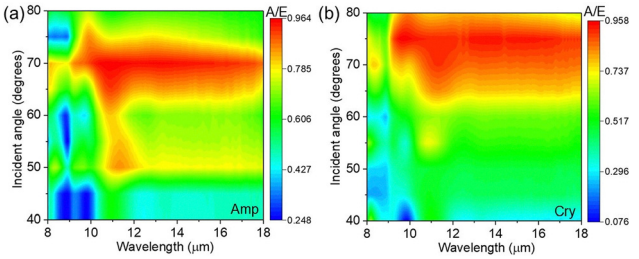

Fig. 3 Measured *p*-polarized angular absorption (*A*)/emissivity (*E*) spectrum of the SiO_2–Sb_2S_3 multilayer when the structural phase of Sb_2S_3 is (a) amorphous and (b) crystalline.

is obtained at a Brewster angle of 70°, while the Brewster angle shifts to 75° for the crystalline cavity. Consequently, the angular range of maximum thermal emission changes from 65°–75° to 70°–80° due to the non-volatile phase change of the Sb_2S_3 layers in the cavity from amorphous to crystalline. This indicates that a narrow angular range of directional thermal emission can be tuned, which aligns well with the simulation results. However, a discrepancy below 10 μm exists between the measured and simulated results, as the optical constants used in the simulation are based on literature values. We also conducted polarized angular reflectance measurements using a SiO_2 substrate as a control experiment, as SiO_2 layers in the SiO_2–Sb_2S_3 cavity absorb light above 5 μm (see Fig. S3, SI). As shown, the obtained absorption spectra differ from those of the SiO_2–Sb_2S_3 cavity, rendering directional thermal emission impossible. This confirms that the realized directional thermal emission for *p*-polarization is due to the Brewster effect in the SiO_2–Sb_2S_3 cavity.

We developed a microheater-integrated multilayer cavity to achieve electrically controlled thermal emission. An optical image of the fabricated microheater-integrated multilayer cavity is shown in Fig. 4a, where the Au-based microheater is initially fabricated on a Si substrate using photolithography, metal deposition, and the standard lift-off process, followed by

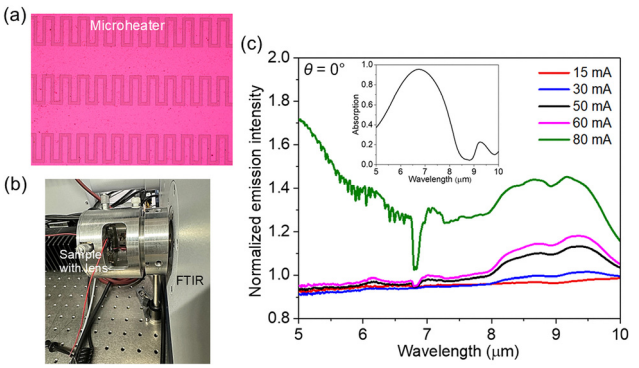

Fig. 4 (a) Optical microscope image of the fabricated microheater-integrated SiO_2–Sb_2S_3 cavity. The array of rectangular patterns represents the Au-based microheater, while the pink color indicates the SiO_2–Sb_2S_3 cavity. (b) Image of the custom-designed experimental setup integrated with the Bruker FTIR. (c) Measured normalized emission intensity at normal incidence for different applied currents; the inset shows the absorption spectrum of the SiO_2–Sb_2S_3 cavity measured at normal incidence.

the deposition of multilayers of Sb_2S_3 and SiO_2. The temperature calibration results of the microheater indicate that the temperature varies linearly with the applied current (see Fig. S4, SI). A custom-designed experimental setup, integrated with the Bruker Fourier-transform infrared (FTIR) spectrometer, is meticulously engineered for high-precision emission measurements at normal incidence (Fig. 4b). This setup incorporates a Cassegrain lens, known for its dual-mirror optical system, which combines a primary parabolic mirror and a secondary hyperbolic mirror to provide a high numerical aperture and efficient light collection over a wide spectral range. The lens is mounted within a specially fabricated, stable lens holder, ensuring precise optical alignment and minimizing potential aberrations or signal losses during measurement. The overall design of the setup is optimized to maximize the signal-to-noise ratio by efficiently collecting and transferring the emitted light, even for samples with low emission intensities. Initially, we measured the emission of the microheater alone to check for any background emission caused by Joule heating and found that the variation in background emission is negligible as the applied current increases (see Fig. S5, SI). We then measured the emission of the microheater-integrated cavity at the same currents and normalized it to the background emission for each current. Fig. 4c shows the normalized thermal emission measured at normal incidence for different applied currents. As observed, the emission intensity gradually increases with the applied current. The emission spectra follow the absorption spectrum of the SiO_2–Sb_2S_3 cavity, measured at normal incidence (inset of Fig. 4c). Significant emission intensity is detected even at an applied current of 80 mA, where the temperature reaches approximately 100 °C, causing the cavity to start emitting. Note that heating below 180 °C does not change the refractive index of the Sb_2S_3 layers. Therefore, the observed emission modulation is solely due to the change in temperature of the microheater. Since the detector is not sensitive enough for longer wavelengths, we cannot extend the emission intensity spectra beyond a 10 μm wavelength.

Tunable directional thermal emission can be further improved by replacing Sb_2S_3 with another lossless phase-change material like $Ge_2Sb_2Se_4Te_1$ (GSST),[35] which offers a higher refractive index contrast than Sb_2S_3 (see Fig. S6, SI). Since the used direct annealing method only changes the phase of the Sb_2S_3 layers from amorphous to crystalline, reconfigurable directional emission cannot be achieved. However, PCM-based multilayer structures can be reconfigured using electrical and optical pulses through a melt-quench process.[36–38] Notably, optical switching enables the proposed thermal emitter to support multi-state switching, allowing for reconfigurable directional thermal emission with multiple cycles, along with a microheater that operates below 180 °C solely for thermal radiation control. The measured reflectance spectrum of the cavity, spanning from visible to near-infrared wavelengths, shows that the cavity has two tunable photonic bandgaps (see Fig. S1, SI). The cavity either reflects or transmits light below 5 μm; thus, absorption is negligible below this wavelength, while thermal emission occurs above 5 μm, which is crucial for developing an efficient daytime radiative cooling coating. Compared to

existing thermo-optic-based tunable directional thermal emitters,[27] the proposed device offers non-volatile, tunable directional control with a broadband response.

4. Conclusions

We demonstrated the tunable directional control of thermal emission using a SiO_2–Sb_2S_3 multilayer-based tunable thermal emitter. We showed that the angular range of maximum emissivity over a broad spectral band can be controlled by utilizing the Brewster angle effect of the SiO_2–Sb_2S_3 multilayer cavity. More importantly, this angular range can be adjusted by leveraging the non-volatile structural phase transition property of Sb_2S_3. Furthermore, we demonstrated that thermal emission can be electrically controlled using a compact microheater-integrated SiO_2–Sb_2S_3 multilayer cavity. This lithography-free active photonic platform has the potential to serve as a dynamically tunable thermal emitter for controlling the directionality of broadband thermal emission.

Author contributions

KVS designed the thermal emitter, performed the simulation, fabricated and characterized the samples, collected and analyzed the results, prepared figures, and wrote the original manuscript draft; QYSW performed FTIR measurements and emission measurements, and collected and analyzed the results; SJ fabricated and characterized the samples; RS corrected the original manuscript; JT initiated and supervised the project and corrected the original manuscript. All the authors contributed to the writing of the manuscript.

Conflicts of interest

The authors declare that they have no conflict of interest.

Data availability

The data supporting this article have been included as part of the SI.

Additional experimental and simulation results. See DOI: **https://doi.org/10.1039/d5nh00367a**

Acknowledgements

J. T. acknowledges the support from the Agency for Science, Technology and Research (A*STAR) under MTC Programmatic Grant (M22L1b0110), the National Research Foundation, Singapore under NRF-CRP (NRF-CRP26-2021-0004), and the National Semiconductor Translation and Innovation Centre (NSTIC).

References

1 D. G. Baranov, Y. Xiao, I. A. Nechepurenko, A. Krasnok, A. Alu and M. A. Kats, Nanophotonic engineering of far-field thermal emitters, *Nat. Mater.*, 2019, **18**, 920.
2 A. P. Raman, M. A. Anoma, L. Zhu, E. Rephaeli and S. Fan, Passive radiative cooling below ambient air temperature under direct sunlight, *Nature*, 2014, **515**, 540–544.
3 L. Cai, A. Y. Song, W. Li, P.-C. Hsu, D. Lin, P. B. Catrysse, Y. Liu, Y. Peng, J. Chen, H. Wang, J. Xu, A. Yang, S. Fan and Y. Cui, Spectrally selective nanocomposite textile for outdoor personal cooling, *Adv. Mater.*, 2018, **30**, 1802152.
4 E. Sakr and P. Bermel, Thermophotovoltaics with spectral and angular selective doped-oxide thermal emitters, *Opt. Express*, 2017, **25**, A880–A895.
5 Y. Wang, H. Ji, B. Liu, P. Tang, Y. Chen, J. Huang, Y. Ou and J. Tao, Radiative cooling: structure design and application, *J. Mater. Chem. A*, 2024, **12**, 9962–9978.
6 S. Zhang, Z. Liu, Z. Wu, Z. Yao, W. Zhang, Y. Zhang, Z. Guan, H. Lin, H. Cheng, E. Mu, J. Zeng, C. Dun, X. Zhang, J. C. Ho and Z. Hu, Boosting self-powered wearable thermoelectric generator with solar absorber and radiative cooler, *Nano Energy*, 2024, **132**, 110381.
7 E. Mu, Z. Wu, Z. Wu, X. Chen, Y. Liu, X. Fu and Z. Hu, A novel self-powering ultrathin TEG device based on micro/nano emitter for radiative cooling, *Nano Energy*, 2019, **55**, 494–500.
8 K. Chamoli, W. Li, C. Guo and M. Elkbbash, Angularly selective thermal emitters for deep subfreezing daytime radiative cooling, *Nanophotonics*, 2022, **11**, 3709–3717.
9 J. Zhou, T. G. Chen, Y. Tsurimaki, A. Hajj-Ahmad, L. Fan, Y. Peng, R. Xu, Y. Wu, S. Assawaworrarit, S. Fan, M. R. Cutkosky and Y. Cui, Angle-selective thermal emitter for directional radiative cooling and heating, *Joule*, 2023, **7**, 2830–2844.
10 Y. Qu, M. Pan and M. Qiu, Directional and spectral control of thermal emission and its application in radiative cooling and infrared light sources, *Phys. Rev. Appl.*, 2020, **13**, 064052.
11 Z. Fan, T. Hwang, S. Lin, Y. Chen and Z. J. Wong, Directional thermal emission and display using pixelated non-imaging micro-optics, *Nat. Commun.*, 2024, **15**, 4544.
12 M. F. Picardi, K. N. Nimie and G. Papadakis, Dynamic modulation of thermal emission—A Tutorial, *J. Appl. Phys.*, 2023, **133**, 111101.
13 T. Inoue, M. De Zoysa, T. Asano and S. Noda, Realization of dynamic thermal emission control, *Nat. Mater.*, 2014, **13**, 928–931.
14 K.-K. Du, Q. Li, Y.-B. Lyu, J.-C. Ding, Y. Lu, Z.-Y. Cheng and M. Qui, Control over emissivity of zero-static-power thermal emitters based on phase-changing material GST, *Light: Sci. Appl.*, 2017, **6**, e16194.
15 L. Wojszvzyk, A. Nguyen, A.-L. Coutrot, C. Zhang, B. Vest and J.-J. Greffet, An incandescent metasurface for quasimonochromatic polarized mid-wave infrared emission modulated beyond 10 MHz, *Nat. Commun.*, 2021, **12**, 1492.
16 G. T. Papadakis, B. Zhao, S. Buddhiraju and S. Fan, Gate-tunable near-field heat transfer, *ACS Photonics*, 2019, **6**, 709–719.

17 R. M. Abraham Ekeroth, P. Ben-Abdallah, J. C. Cuevas and A. García-Martín, Anisotropic thermal magnetoresistance for an active control of radiative heat transfer, *ACS Photonics*, 2018, **5**, 705–710.
18 L. Ge, Z. Xu, Y. Cang and K. Gong, Modulation of near-field radiative heat transfer between graphene sheets by strain engineering, *Opt. Express*, 2019, **27**, A1109–A1117.
19 Z. Wu, Z. Wu, H. Lv, W. Zhang, Z. Liu, S. Zhang, E. Mu, H. Lin, Q. Zhang, D. Cui, T. Thundat and Z. Hu, Nanophotonic catalytic combustion enlightens mid-infrared light source, *Nano Res.*, 2023, **16**, 11564–11570.
20 J. Xu, J. Mandal and A. P. Raman, Broadband directional control of thermal emission, *Science*, 2021, **372**, 393–397.
21 J. S. Hwang, J. Xu and A. P. Raman, Simultaneous control of spectral and directional emissivity with gradient epsilon-near-zero InAs photonic structures, *Adv. Mater.*, 2023, **35**, 2302956.
22 Y. Ma, J. Wang, L. Li, T. Liu and W. Li, Broadband unidirectional thermal emission, *Laser Photonics Rev.*, 2025, **19**, 2400716.
23 J. Yu, R. Qin, Y. Ying, M. Qiu and Q. Li, Asymmetric directional control of thermal emission, *Adv. Mater.*, 2023, **35**, 2302478.
24 Q. Chen, C. Li, X. Huang, Y. Lu, H. Xu, Y. An, L. Li, W. Li, X. Yin, X. Cao and D. Zhao, Ultrabroadband directional tunable thermal emission control based on vanadium dioxide photonic structures, *Adv. Sci.*, 2025, **12**, 2416437.
25 Y. Wang, H. Ji, Y. Chen, B. Liu, J. Huang, M. Lu, Y. Ou, Y. Zhao, J. Tao, Y. Huang and J. Wang, Artificially adjustable radiative cooling device with environmental adaptability, *Ceram. Int.*, 2023, **49**, 40297–40304.
26 Y. Zhao, H. Ji, Y. Ou, Y. Wang, Y. Chen, J. Tao, B. Liu, M. Lu, Y. Huang and J. Wang, Novel sunlight-driven Cu_7S_4/VO_2 composite films for smart windows, *J. Mater. Chem. C*, 2024, **12**, 2534–2543.
27 J. S. Hwang, J. Xu and A. P. Raman, Thermally tunable angular selectivity of broadband directional thermal emission, *Nano Lett.*, 2025, **25**, 8064–8071.
28 M. Wuttig, H. Bhaskaran and T. Taubner, Phase-change materials for non-volatile photonic applications, *Nat. Photon.*, 2017, **11**, 465–476.
29 K. V. Sreekanth, C. M. Das, R. Medwal, M. Mishra, Q. Ouyang, R. S. Rawat, K. T. Yong and R. Singh, Electrically tunable singular phase and Goos–Hänchen shifts in phase-change-material-based thin-film coatings as optical absorbers, *Adv. Mater.*, 2021, **33**, 2006926.
30 A. Biegański, M. Perestjuk, R. Armand, A. D. Torre, C. Laprais, G. Saint-Girons, V. Reboud, J.-M. Hartmann, J.-H. Tortai, A. Moreau, J. Lumeau, T. Nguyen, A. Mitchell, C. Monat, S. Cueff and C. Grillet, Sb_2S_3 as a low-loss phase-change material for mid-IR photonics, *Opt. Mater. Express*, 2024, **14**, 862–870.
31 K. V. Sreekanth, J. Perumal, U. S. Dinish, P. Prabhathan, Y. Liu, R. Singh, M. Olivo and J. Teng, Tunable Tamm plasmon cavity as a scalable biosensing platform for surface enhanced resonance Raman spectroscopy, *Nat. Commun.*, 2023, **14**, 7085.
32 K. V. Sreekanth, S. Jana, Q. Y. S. Wu, M. Zhao, R. Singh and J. Teng, Dual-phase singularity at a single incident angle with spectral tunability in Tamm cavities, *Adv. Mater.*, 2024, **36**, 2408098.
33 P. Yeh, A. Yariv and C.-S. Hong, Electromagnetic propagation in periodic stratified media. I. General Theory, *J. Opt. Soc. Am.*, 1977, **67**, 423–438.
34 J. Kischkat, S. Peters, B. Gruska, M. Semtsiv, M. Chashnikova, M. Klinkmüller, O. Fedosenko, S. Machulik, A. Aleksandrova, G. Monastyrskyi, Y. Flores and W. T. Masselink, Mid-infrared optical properties of thin films of aluminum oxide, titanium dioxide, silicon dioxide, aluminum nitride, and silicon nitride, *Appl. Opt.*, 2012, **51**, 6789–6798.
35 Y. Zhang, J. B. Chou, J. Li, H. Li, Q. Du, A. Yadav, S. Zhou, M. Y. Shalaginov, Z. Fang, H. Zhong, C. Roberts, P. Robinson, B. Bohlin, C. Ríos, H. Lin, M. Kang, T. Gu, J. Warner, V. Liberman, K. Richardson and J. Hu, Broadband transparent optical phase change materials for high-performance nonvolatile photonics, *Nat. Commun.*, 2019, **10**, 4279.
36 Y. Wang, P. Landreman, D. Schoen, K. Okabe, A. Marshall, U. Celano, H.-S. P. Wong, J. Park and M. L. Brongersma, Electrical tuning of phase-change antennas and metasurfaces, *Nat. Nanotechnol.*, 2021, **16**, 667–672.
37 S. Jana, K. V. Sreekanth, O. A. M. Abdelraouf, R. Lin, H. Liu, J. Teng and R. Singh, Aperiodic Bragg reflectors for tunable high-purity structural color based on phase change material, *Nano Lett.*, 2024, **24**, 3922–3929.
38 D. Lawson, S. Blundell, M. Ebert, O. L. Muskens and I. Zeimpekis, Optical switching beyond a million cycles of low-loss phase change material Sb_2Se_3, *Opt. Mater. Express*, 2024, **14**, 22–38.

